Optics Letters

Quartz tuning fork embedded off-beam quartz-enhanced photoacoustic spectroscopy

Lien Hu,[1] Chuantao Zheng,[1,*] Jie Zheng,[1] Yiding Wang,[1] and Frank K. Tittel[2]

[1]*State Key Laboratory of Integrated Optoelectronics, College of Electronic Science and Engineering, Jilin University, Changchun 130012, China*
[2]*Department of Electrical and Computer Engineering, Rice University, Houston, Texas 77005, USA*
Corresponding author: zhengchuantao@jlu.edu.cn

In order to achieve a high acoustic coupling strength and detection sensitivity and to simplify the assembly and alignment process in quartz-enhanced photoacoustic spectroscopy (QEPAS) technique, a novel quartz tuning fork (QTF) embedded off-beam QEPAS (E-OB-QEPAS) spectrophone was proposed. The structural parameters of the acoustic micro-resonator of the E-OB-QEPAS spectrophone were optimized for enhancing the signal-to-noise ratio gain based on experimental investigation. Compared with the on-beam configuration using a bare QTF, a detection sensitivity enhancement by a factor of ~25 was achieved by embedding the QTF in one resonant tube. By using two resonant tubes simultaneously embedded with a QTF, dual-channel detection and a two-fold photoacoustic signal enhancement were realized and a detection sensitivity enhancement by a factor of ~20 and ~40 were achieved for the single-tube-enhanced and dual-tube-enhanced E-OB-QEPAS spectrophone, respectively. © 2019 Optical Society of America

Quartz-enhanced photoacoustic spectroscopy (QEPAS) is a rapidly developing photoacoustic spectroscopy technique for trace gas detection since its first introduction in 2002 [1]. As an alternative approach for photoacoustic detection, by using a quartz tuning fork (QTF) instead of a microphone as a sharply resonant acoustic transducer, QEPAS reveals some comprehensive properties, including high sensitivity with a small sensing module, wide dynamic range, excitation wavelength independence, and immunity to environmental acoustic noise [2,3].

An acoustic micro-resonator (AmR) was usually utilized to improve the performance of a QEPAS sensor [4]. An AmR-based QTF is referred to as a QEPAS spectrophone. The common on-beam configuration, with difficulty in assembly and alignment, realizes a strong acoustic coupling between the resonant tube and the QTF and achieves a detection sensitivity enhancement by a factor of ~30 using a standard commercial QTF [5,6]. The single-tube on-beam QEPAS (SO-QEPAS) is effective to obtain a stronger acoustic coupling than the common on-beam configuration owing to the reduced acoustic leakage between QTF prongs [7]. However, this configuration cannot be employed by a commercial QTF with a small gap of ~0.3 mm between the prongs. Another spectrophone configuration named off-beam QEPAS was first proposed in 2009 [8]. The common off-beam configuration is technologically easier to assemble and align than the common on-beam configuration; however, a relatively weak resonant tube to QTF coupling leads to a long response time [2,9,10] and its detection sensitivity enhancement by a factor of ~19 is lower than the on-beam configuration [2]. Compared with the common off-beam QEPAS, the sensitivity enhancement factor for the T-tube off-beam QEPAS was increased to ~30 [11]; but the T-tube processing was more complex than the traditional resonant tube and also the acoustic coupling was weak.

In order to achieve a high acoustic coupling strength and detection sensitivity and to simplify the assembly and alignment process in QEPAS, we aim to propose a new spectrophone configuration based on a standard commercial QTF. This spectrophone configuration is named as QTF embedded off-beam QEPAS (E-OB-QEPAS).

The schematics of the E-OB-QEPAS spectrophone with one or two resonant tubes are shown in Figs. 1(a)–1(c). There is a slit located in the middle of the tube and the QTF plane is embedded in the slit. A right-angle prism can be employed in the dual-tube configuration for light reflection as shown in Fig. 1(b) [12]. Meanwhile, if the laser beam is not reflected back to another tube, as shown in Fig. 1(c), a double-channel detection can be realized. This configuration is suitable for a simultaneous detection of two gas species based on time-division multiplexing (TDM) technique without the combination of laser beams. The definition of the geometrical parameters of the E-OB-QEPAS spectrophone with one and two resonant tubes is shown in Figs. 1(d) and 1(e). The length of the resonant tube is L. The depth and width of the slit are d and w, respectively. ID and OD are the inner and outer diameter of the resonant tube, respectively. The vertical distance between the opening of the QTF and the axis of the resonant tube is h, which is set to ~1 mm [9]. In the preliminary experiment, d and w are set to 0.6 mm and 0.4 mm, respectively. The outer diameter is set to OD = 1.2 mm, leading to a gap of ~150 μm in the x direction (x-gap) and a gap of ~80 μm in the z direction (z-gap).
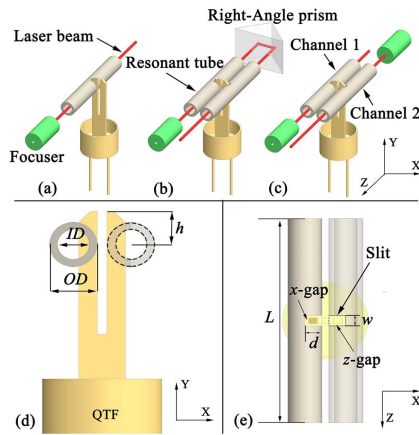
Fig. 1. Schematic of the E-OB-QEPAS spectrophone. (a) Single-tube E-OB-QEPAS spectrophone with one prong for detection. (b) Dual-tube-enhanced E-OB-QEPAS spectrophone with two prongs for detection. (c) Dual-tube dual-channel E-OB-QEPAS spectrophone. (d–e) Definition of the geometrical parameters of the E-OB-QEPAS spectrophone.

The performance of the proposed E-OB-QEPAS configuration with one and two resonant tubes was maximized by optimizing ID and L. A diagram of the experiment setup is shown in Fig. 2. The resonant frequency f_0 and the quality factor (Q-factor) of the QTF were determined via an electric excitation method [10]. The resonant frequency is ~32.760 kHz. A fiber-coupled distributed feedback (DFB) diode laser was used to target a H_2O absorption line at ~7306.75 cm^{-1} with a line intensity of 1.8×10^{-20} $cm \cdot mol^{-1}$ obtained from the high-resolution transmission (HITRAN) molecular absorption spectra database. The diode laser was controlled by a commercial temperature controller (Thorlabs, Model TED 200C) and a laser current driver (Thorlabs, Model LDC202C). The laser beam was focused to pass through the AmR by a fiber-coupled focuser (OZ optics Ltd., Model LPF-05). The piezoelectric current of the QTF was converted to voltage by a trans-impedance amplifier. The voltage signal was demodulated at f_0 by a lock-in amplifier (Stanford Research System, Model SR830). The time constant of the lock-in amplifier and the slope filter were set to 1 s and 18 dB/octave, respectively, leading to a detection bandwidth of $\Delta f = 0.094$ Hz.
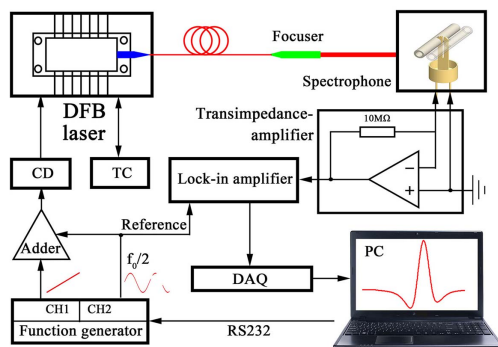

Fig. 2. Experiment setup of the E-OB-QEPAS system by utilizing a fiber-coupled DFB diode laser at 7306.75 cm^{-1} for water vapor detection. CD: laser current driver; TC: laser temperature controller; DAQ: data acquisition card; PC: personal computer.

Four single-tube E-OB-QEPAS spectrophones (AmR1–AmR4) and a dual-tube E-OB-QEPAS spectrophone (AmR5) were fabricated and the corresponding parameters are listed in Table 1. The Q-factors Q_a with different AmRs and Q-factors Q_b of bare QTFs were measured for evaluating the acoustic coupling strength and detection sensitivity enhancement factor [5]. The sensitivity enhancement factor is determined by the signal-to-noise ratio gain (SNR Gain), expressed as [11]

$$\text{SNR Gain} = \text{Signal Gain} \times \sqrt{Q_b/Q_a}. \qquad \textbf{(1)}$$

The Signal Gain is defined as the ratio of the normalized QTF signal intensity between the E-OB-QEPAS spectrophone and on-beam QEPAS with a bare QTF [8]. The H_2O concentration was determined by a direct laser absorption spectroscopy with a 30 cm-long optical path. The output laser power was measured to be ~8 mW at the target H_2O absorption wavelength.

The Signal Gain, Q_a, and SNR Gain as a function of the tube length for AmR1 are shown in Fig. 3. A stronger acoustic coupling leads to a decrease in the Q-factor because the high-Q QTF transfers energy primarily via the coupling to the low-Q AmR oscillator [9]. As the tube length decreases, the coupling between the resonant tube and the QTF first increases and then decreases. When the one-dimensional longitudinal resonant frequency of the tube is equal to the resonant frequency of the QTF, the Q-factor reaches to the minimum value [13]. The enhanced coupling increases the sound pressure intensity detected by the QTF, resulting in a resonant enhancement but reduction in the piezoelectric conversion rate of the QTF, because the QTF signal amplitude is proportional to the magnitude of the Q-factor [14]. These two factors generate the maximum photoacoustic signal and the maximum Signal Gain. However, with the resonant tube length continues to decrease, although the Q-factor increases gradually, the Signal Gain continues to decrease because the restriction of the resonant tube on acoustic wave is weakened due to the too short resonant tube. For maximizing the SNR Gain, the optimal tube length (8.4 mm for AmR1) is within the range from the tube length corresponding to the peak value of Signal Gain (9.0 mm for AmR 1) to the tube length corresponding to the valley value of Q_a (8.0 mm for AmR1).

The SNR Gain as a function of the tube length for AmR1–AmR4 were optimized and depicted in Fig. 4(a). The maximum SNR Gain for AmR1, AmR2, AmR3, and AmR4 were obtained at the length of 8.4 mm, 8.4 mm, 8 mm, and 7.8 mm, respectively. Generally, the optimal length and the SNR gain increase with the decrease of the inner diameter, because a longer resonant tube with a smaller inner diameter is helpful to the accumulation of acoustic energy. The optimal SNR Gain as a function of the inner diameter is shown in Fig. 4(b). A linear fitting with an R-square value of >0.977 indicates that the optimal SNR gain increases linearly with the decrease of the inner diameter. In order to obtain a larger SNR Gain, a tube with a smaller inner diameter is expected. However, an inner diameter that is too small will increase the difficulty in system assembly and lead to a high requirement of beam quality.

Two independent channels can be used for the dual-tube E-OB-QEPAS spectrophone. The SNR Gain as a function of the tube length for channel 1, channel 2, and channel 1&2 [achieved by a right-angle prism, see Fig. 1(b)] acquired by the dual-tube E-OB-QEPAS spectrophone AmR5 are

Table 1.   Design Parameters and Optimized Results for Different AmRs

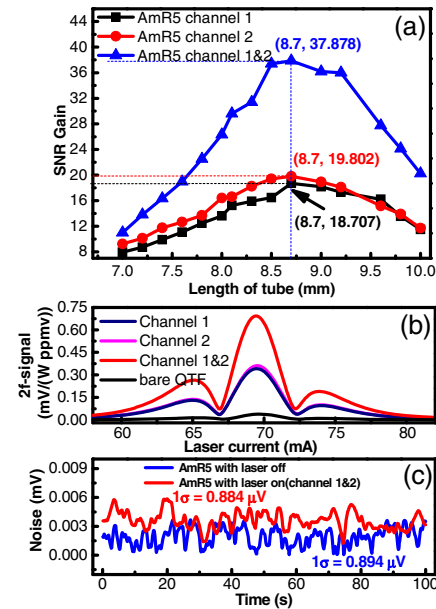| AmRs	Parameter (mm)				QTF Signal (mV)	C(H₂O)	Normalized QTF Signal Intensity (mV/(W ppmv))	Signal Gain	SNR Gain
	ID	L	Q_b	Q_a					
AmR1	0.6	8.4	11761	4145	38.38	0.846%	0.567	14.942	25.169
AmR2	0.65	8.4	10210	3646	51.14	1.244%	0.514	13.535	22.650
AmR3	0.8	8	10382	4705	18.99	0.670%	0.368	9.689	14.392
AmR4	0.87	7.8	11401	5455	20.74	0.770%	0.337	8.875	12.831
AmR5(dual-tube)	0.6	8.7	11320	2608	44.91[c]	0.810%	0.690	18.181	37.878
					22.56[b]	0.780%	0.361	9.505	19.802
					21.39[a]	0.780%	0.341	8.979	18.707
Common on-beam QEPAS without acoustic micro-resonator[d]			10765	–	4.94	1.630%	0.038	1	1

[a]Channel 1.
[b]Channel 2.
[c]Channel 1&2 (dual-tube enhanced) for dual-tube E-OB-QEPAS spectrophone AmR5.
[d]The data was measured based on the on-beam QEPAS with a bare QTF and the laser beam was ~0.7 mm below the opening of the QTF to maximize the QTF signal.
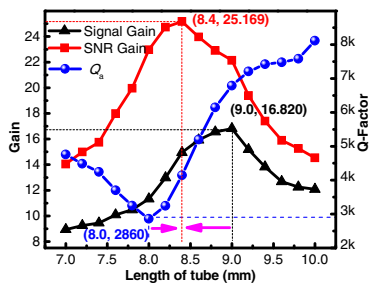
Fig. 3. Signal Gain, Q-factor Q_a, and SNR Gain as a function of the tube length for the single-tube E-OB-QEPAS spectrophone AmR1.
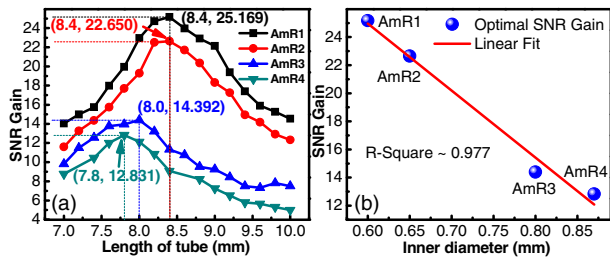
Fig. 4. (a) SNR Gain as a function of the tube length for the single-tube E-OB-QEPAS spectrophones AmR1–AmR4. (b) Optimal SNR Gain as a function of the inner diameter of the tube.

Fig. 5. (a) SNR Gain as a function of the tube length for AmR5. (b) Normalized $2f$-signal for AmR5 and bare QTF (on-beam configuration). (c) Noise generated by the dual-tube E-OB-QEPAS spectrophone (channel 1&2 of AmR5) with laser on and off, where the laser emitting wavelength doesn't target the water absorption line.

shown in Fig. 5(a). The optimal lengths for channel 1, channel 2, and channel 1&2 are equal, i.e., 8.7 mm. Although the inner diameters of the resonant tubes used in AmR1 and AmR5 are identical, the optimal lengths for AmR5 are a bit larger than the optimal length for AmR1. This slight increase results probably from an increased viscous loss, which is derived from the viscous drag force exerted on the vibrating beam by the surrounding medium (i.e., air) [2]. Compared to AmR1, the viscous drag for AMR5 gets larger because of using two resonant tubes and dampens the QTF vibration. Thus, the increased viscous

loss leads to a decreased SNR Gain from ~25 (AmR1) to ~20 for the single-tube-enhanced dual-tube E-OB-QEPAS spectrophone (AmR5). The SNR Gain for channel 1&2 was close to the sum of the SNR Gain of channel 1 and channel 2, generating a dual-tube-enhanced E-OB-QEPAS spectrophone.

The optimized results for AmR1 to AmR5 are listed in Table 1. The Q-factor of a QTF encapsulated in vacuum is 20,000 or higher and decreases to ~10,000 (Q_b) when the QTF is in the air with a 1 atm pressure due to the viscous loss. The Q-factor changes from $Q_b \sim 10,000$ to $Q_a \sim 4,000$ for AmR1, resulting in a stronger acoustic coupling than other off-beam QEPAS (Common off-beam: $Q_b \sim 13,000$,

$Q_a \sim 7,000$ [2]; T-tube off-beam: $Q_b \sim 9,000$ to $Q_a \sim 5,000$ [11]). When two resonant tubes were employed, the Q-factor was further reduced to $\sim 2,600$ for AmR5, and a similar acoustic coupling strength was achieved in the common on-beam QEPAS ($Q_b \sim 10,000$ (bare QTF), $Q_a \sim 2,500$ [5]). The decrease of the Q-factor is attributed to a high measurement pressure and the increased acoustic coupling. Besides, since the response time of a QTF is determined by $Q_a/(\pi f_0)$ [9], the decrease of Q_a speeds up the QTF response and allows for rapid spectral measurement.

Generally, based on Fig. 3 and Eq. (1), a proper strong acoustic coupling enhances the normalized QTF signal intensity and decreases the quality factor. However, the minimum Q_a does not mean the maximum Signal Gain, which indicates that the maximum SNR Gain is a comprehensive effect of the decrease of the quality factor and the enhancement of the normalized QTF signal intensity. As a comparison, the dual-tube-enhanced E-OB-QEPAS has a higher Signal Gain (~ 18.2) and a stronger acoustic coupling ($Q_b/Q_a \sim 4.3$) than the common on-beam QEPAS with a Signal Gain of ~ 15 and a Q_b/Q_a of ~ 4 [5], leading to a SNR gain enhancement of ~ 1.3. The reported common off-beam QEPAS has a Signal Gain of ~ 14.4 and a Q_b/Q_a of ~ 1.69 [2], resulting in a SNR Gain of only ~ 19, which is ~ 2 times smaller compared to the dual-tube-enhanced E-OB-QEPAS. The proposed single-tube E-OB-QEPAS has a lower SNR Gain (~ 25) than the common on-beam QEPAS and the T-tube off-beam QEPAS with a SNR Gain of ~ 30. Compared to the common off-beam QEPAS, this single-tube E-OB-QEPAS has a higher SNR Gain by a factor of ~ 1.3.

Using the same resonate tube with an ID of 600 μm, in the common off-beam and E-OB-QEPAS, the laser beam should pass through a ~ 600 μm and ~ 450 μm (ID/2 + x-gap) gap, respectively. So, the alignment and assembly process of the E-OB-QEPAS seems to be a bit more complex. For the common on-beam QEPAS, (1) the two tubes and the QTF should be seriously on-beam, which requires more steps in the assembly process; (2) The laser beam passing through a ~ 300 μm gap is a bit more difficult for aligning than the E-OB-QEPAS, which requires the laser beam passing through a ~ 450 μm gap.

Figure 5(b) shows the normalized second harmonic signal ($2f$-signal) for channel 1, channel 2, and channel 1&2 of AmR5. A similar normalized photoacoustic signal intensity was observed for channel 1 and channel 2. The signal intensity of channel 1&2 was close to the sum of channel 1 and channel 2, leading to a two-fold SNR Gain. The background noise for channel 1&2 was measured by tuning the laser emitting wavelength to be far away from the H_2O absorption line. In addition, the noise without laser beam passing through the AmR (i.e., the laser is turned off) was also measured. As shown in Fig. 5(c), the standard deviations of the background noise under the two cases have a similar level, which were 0.884 and 0.894 μV, respectively. Therefore, there was no extra noise introduced by the laser radiation and the noise level can be determined by the thermal excitation of the QTF [5,8,11,15]. The theoretical thermal noise level of the QTF was ~ 0.51 μV, based on a measured serial resistor of ~ 600 kΩ and an assumed temperature of 293 K. The measured noise level was slightly larger than the theoretical thermal noise, probably resulting from the noise of the transimpedance amplifier. The $2f$-signal

amplitude for the optimized AmR5-based dual-tube-enhanced spectrophone was 44.91 mV with a H_2O concentration of 0.810% at a 1 atm pressure and temperature of ~ 293 K, leading to a SNR of ~ 50803. Therefore, the sensor reveals the minimum detectable concentration of 0.159 parts per million in volume (ppmv) and a normalized noise equivalent absorption coefficient, $\text{NNEA}(1\sigma) = 6.59 \times 10^{-9}$ $\text{cm}^{-1}\,\text{W}/\sqrt{\text{Hz}}$.

In conclusion, we proposed a novel off-beam QEPAS spectrophone by embedding a standard commercial QTF in one or two resonant tubes. The advantages of the structure are summarized as: (1) the E-OB-QEPAS increases the sensing area of the QTF prongs by embedding the QTF partially inside the resonant tube; (2) the sensitivity can be increased by an optimally enhanced acoustic coupling and by using the dual-tube configuration with dual-prong for detection; (3) it is easy to fabricate the tube with only making a slit; the alignment and assembly process simply requires the laser beam propagation through a gap without the need to seriously align the QTF and the tube. A detailed optimization of the slit size and outer diameter of the resonant tube is expected to enhance the detection sensitivity.

REFERENCES

1. A. A. Kosterev, Y. A. Bakhirkin, R. F. Curl, and F. K. Tittel, Opt. Lett. **27**, 1902 (2002).
2. K. Liu, H. Yi, A. A. Kosterev, W. Chen, L. Dong, L. Wang, T. Tan, W. Zhang, F. K. Tittel, and X. Gao, Rev. Sci. Instrum. **81**, 103103 (2010).
3. P. Patimisco, A. Sampaolo, L. Dong, F. K. Tittel, and V. Spagnolo, Appl. Phys. Rev. **5**, 011106 (2018).
4. P. Patimisco, G. Scamarcio, F. K. Tittel, and V. Spagnolo, Sensors **14**, 6165 (2014).
5. L. Dong, A. A. Kosterev, D. Thomazy, and F. K. Tittel, Appl. Phys. B **100**, 627 (2010).
6. H. Wu, A. Sampaolo, L. Dong, P. Patimisco, X. Liu, H. Zheng, X. Yin, W. Ma, L. Zhang, W. Yin, V. Spagnolo, S. Jia, and F. K. Tittel, Appl. Phys. Lett. **107**, 111104 (2015).
7. H. Zheng, L. Dong, A. Sampaolo, H. Wu, P. Patimisco, X. Yin, W. Ma, L. Zhang, W. Yin, V. Spagnolo, S. Jia, and F. K. Tittel, Opt. Lett. **41**, 978 (2016).
8. K. Liu, X. Guo, H. Yi, W. Chen, W. Zhang, and X. Gao, Opt. Lett. **34**, 1594 (2009).
9. L. Dong, H. Wu, H. Zheng, Y. Liu, X. Liu, W. Jiang, L. Zhang, W. Ma, W. Ren, W. Yin, S. Jia, and F. K. Tittel, Opt. Lett. **39**, 2479 (2014).
10. A. A. Kosterev, P. R. Buerki, L. Dong, M. Reed, T. Day, and F. K. Tittel, Appl. Phys. B **100**, 173 (2010).
11. H. Yi, W. Chen, S. Sun, K. Liu, T. Tan, and X. Gao, Opt. Express **20**, 9187 (2012).
12. Y. Liu, J. Chang, J. Lian, Z. Liu, Q. Wang, and Z. Qin, Sensors **16**, 214 (2016).
13. Y. Cao, W. Jin, and H. L. Ho, Sens. Actuators B **174**, 24 (2012).
14. H. Wu, L. Dong, H. Zheng, Y. Yu, W. Ma, L. Zhang, W. Yin, L. Xiao, S. Jia, and F. K. Tittel, Nat. Commun. **8**, 15331 (2017).
15. N. Petra, J. Zweck, A. A. Kosterev, S. E. Minkoff, and D. Thomazy, Appl. Phys. B **94**, 673 (2009).